

# Recent developments in compact ultrafast lasers

Ursula Keller

Physics Department, Swiss Federal Institute of Technology (ETH), Zürich, Switzerland (e-mail: [keller@phys.ethz.ch](mailto:keller@phys.ethz.ch))

Ultrafast lasers, which generate optical pulses in the picosecond and femtosecond range, have progressed over the past decade from complicated and specialized laboratory systems to compact, reliable instruments. Semiconductor lasers for optical pumping and fast optical saturable absorbers, based on either semiconductor devices or the optical nonlinear Kerr effect, have dramatically improved these lasers and opened up new frontiers for applications with extremely short temporal resolution (much smaller than 10 fs), extremely high peak optical intensities (greater than 10 TW/cm<sup>2</sup>) and extremely fast pulse repetition rates (greater than 100 GHz).

**S**ix years after the first laser was demonstrated, De Maria and co-workers produced the first ultrashort pulses, estimated to be just picoseconds long, using a passively modelocked Nd:glass laser<sup>1</sup>. Modelocking is a technique that generates ultrashort pulses from lasers. We distinguish between active and passive modelocking, and the latter can generate much shorter pulses using saturable absorbers.

The result from De Maria *et al.*<sup>1</sup> had an underlying problem: it did not measure a regular pulse train as described in Box 1. They actually measured an amplitude-modulated pulse train (Fig. 1). In this regime, called Q-switched mode-locking, the modelocked picosecond pulses are modulated with a much longer Q-switched pulse envelope, which occurs at a much lower repetition rate. Lack of a regular pulse train remained a problem for passively modelocked solid-state lasers for more than 20 years.

Eventually the problem was solved in 1992 by using saturable absorbers from semiconductors<sup>2</sup>. Since their introduction, the pulse durations, average powers, pulse energies and pulse repetition rates of compact ultrafast solid-state lasers have improved by several orders of magnitude through the addition of a saturable semiconductor cavity laser mirror (generally referred to as semiconductor saturable absorber mirrors, SESAMs)<sup>2-4</sup>.

Compact efficient semiconductor diode lasers replaced inefficient lamps for optical excitation. Such diode-pumped solid-state lasers have further enhanced reliability and produced unsurpassed performance. For ultrabroadband tunability and to produce even shorter pulses, a faster, saturable absorber mechanism, referred to as Kerr lens modelocking<sup>5</sup>, is required. Currently, pulse durations can range from picoseconds to a few femtoseconds, depending on the laser material and the parameters of the saturable absorber. The average power has been increased to 60 W directly from a modelocked diode-pumped laser with pulse energies larger than 1 mJ<sup>6</sup>, and the pulse repetition rate has been increased to more than 100 GHz<sup>7</sup>. These improvements in performance of ultrashort lasers keep advancing the frontiers of ultrashort pulse durations, high average power and high pulse repetition rates, which will be discussed in more detail in this review. But first we continue with an overview of significant applications and a more detailed explanation of the two key enabling technologies, Kerr lens modelocking and semiconductor saturable absorbers. At this point, I believe that the development of ultrafast lasers has not come to its end but will continue to deliver superior performance for many applications.

## Applications of ultrafast lasers

Ultrafast laser technology has developed rapidly over the past decade, and as our understanding develops so will the application of these lasers. By examining four features of ultrafast lasers, I will highlight some of the applications that benefit from laser development.

### Ultrashort pulse duration

Ultrashort pulse duration allows fast temporal resolution. In the same way that a strobe light at a disco 'freezes' the motion of dancers, a modelocked laser can 'freeze' the motion of fast-moving objects such as molecules or electrons and therefore can measure the relaxation processes of carriers in semiconductors<sup>8</sup>, chemical reaction dynamics<sup>9,10</sup> and electro-optical sampling of high-speed electronics<sup>11,12</sup>. Using modelocked lasers, the dissociation dynamics of molecules and more complex chemical reaction dynamics have been measured, and this work was rewarded with a Nobel prize in chemistry for A. H. Zewail in 1999.

### High pulse repetition rate

Lasers with multi-gigahertz repetition rates are key components of many applications. They are used in high-capacity telecommunication systems<sup>13,14</sup>, photonic switching devices<sup>15</sup>, optical interconnections and for clock distribution. And applications of the future such as clocks for very large scale integrated (VLSI) microprocessors<sup>16</sup>, polarized electron beams<sup>17</sup> for electron accelerators and high-speed electro-optic sampling techniques<sup>11,12</sup> will rely on multi-gigahertz pulse trains with short pulses, low timing jitter and low amplitude noise.

As data transmission rates increase, modelocked lasers with a tunable wavelength of around 1.55  $\mu\text{m}$  will become important in telecommunications. Transmission systems at 10 GHz and higher often use return-to-zero (RZ) pulse formats and soliton dispersion management techniques<sup>14,18</sup>. These approaches benefit from the availability of simple, compact, transform-limited optical pulse generators<sup>19,20</sup>. For example, they eliminate the need for a modulator to create the pulses and thereby simplify system architecture, increase efficiency and reduce cost. Additionally, pulse quality is typically very good—much better than with modulated CW (continuous wave) sources. This improves system signal-to-noise ratios and allows scaling to higher repetition rates through optical time-division multiplexing. Transmission of data at 160 Gbits per second through standard single-mode fibres has been demonstrated using such laser sources.

High average power 10–100 GHz sources at shorter wavelengths (for example, 1  $\mu\text{m}$  and below) are promising sources

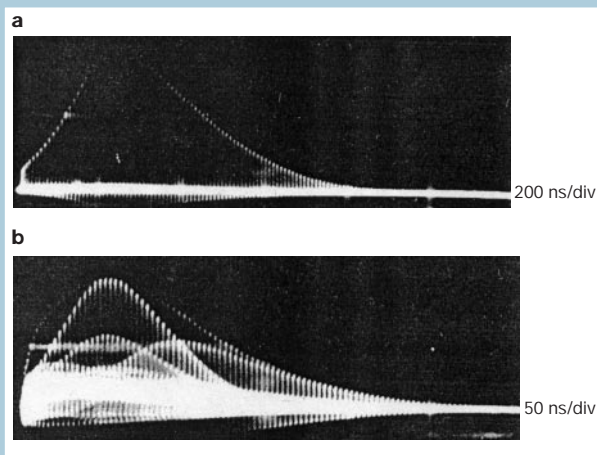


**Figure 1** Pulses from a passively modelocked Nd:glass laser with a dye saturable absorber inside the laser resonator. Picosecond pulses were superimposed upon much longer pulses, which is referred to as Q-switched modelocking. Reprinted with permission from ref. 1 © American Institute of Physics.

for optical clocks in integrated circuits. Current microprocessor clocks in personal computers operate at more than 3 GHz rates, increasing between 15% to 30% annually. The International Technology Roadmap for Semiconductors 2001 (ITRS) forecasts predict a 40 GHz clock rate in 2020. Optical clocks, produced for example by a modelocked laser, can be precisely injected into specific circuits inside a VLSI microprocessor and have the potential to reduce on-chip power requirements, skew, jitter, and support scaling to high clock rates beyond 40 GHz.

#### Broad spectrum

A broad spectrum supports good spatial resolution for optical coherence tomography (OCT), a technique for non-invasive cross-sectional imaging in biological systems<sup>21,22</sup>. OCT uses low coherence interferometry to produce a two-dimensional (2D) image of optical scattering from internal tissue microstructures; this process is similar to that of ultrasonic pulse-echo imaging. OCT does not necessarily need short pulses, but modelocked femtosecond lasers, alone or with additional external spectral broadening, offer a much higher average power than any other broadband source. Thus, these lasers produce a longitudinal and lateral spatial resolution of a few micrometres.

Pulse trains not only provide a broad spectrum but also a stable comb-shaped optical spectrum, where the spacing of the individual longitudinal modes exactly equals the pulse repetition rate (Box 1). Therefore, these lasers are stable multi-wavelength sources<sup>23,24</sup>. The optical comb can be locked to the International Telecommunication Union grid, resulting in a novel multi-wavelength source that is suitable for dense wavelength-division-multiplexing (DWDM) applications<sup>25</sup>.

More recently, the broadband frequency comb has been used for high precision optical frequency metrology<sup>26–28</sup>. The frequency comb produces a ‘ruler’ in the frequency domain with which an unknown optical frequency can be measured. The frequency of the beat (the difference in frequency between the unknown frequency and the closest frequency in the ruler) is always smaller than one half of the comb period. Thus, an optical frequency in the 100 THz regime can be scaled down to a microwave frequency in the range of 1 GHz, which can be measured very accurately. This approach can be used for an all-optical atomic clock that is expected to outperform today’s state-of-the-art caesium clocks<sup>29</sup>.

These broadband frequency combs can also be used to stabilize the electric field underneath the pulse envelope<sup>30,31</sup>, which is important in highly nonlinear processes such as photoionization<sup>32</sup> and

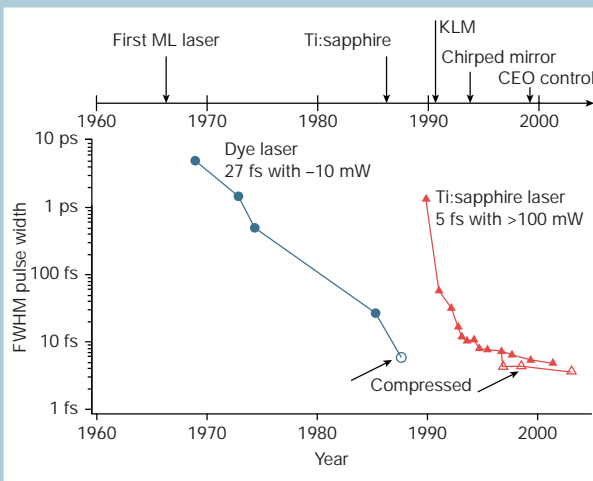


**Figure 2** Improvements in ultrashort pulse generation since the first demonstration of a laser in 1960. Until the end of the 1980s, ultrashort pulse generation was dominated by dye lasers, and pulses as short as 27 fs with an average power of  $\approx 10$  mW were achieved at a centre wavelength of 630 nm (ref. 61). External pulse compression ultimately resulted in pulses as short as 6 fs—a world record result by C. V. Shank’s group that was not surpassed for about 10 years<sup>53</sup>. This situation changed with the discovery of the Ti:sapphire laser. Today, pulses with only two optical cycles at FWHM (full-width half-maximum) at a centre wavelength of 800 nm have been generated with Ti:sapphire lasers with more than 100 mW average output power<sup>52,72</sup>. External compression resulted in pulses as short as 3.8 fs (ref. 76). The filled symbols indicate results directly achieved from a laser; open symbols indicate results achieved with additional external pulse compression.

high-harmonic generation<sup>33</sup>. Such stabilized pulses can support single attosecond pulses in the soft X-ray spectral region<sup>33,34</sup>.

#### High peak intensity

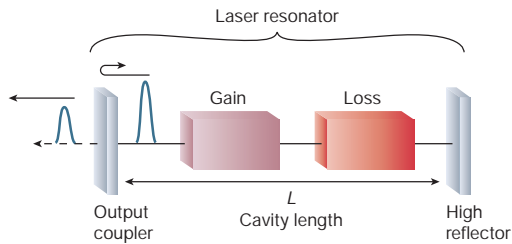
The high peak intensity of the pulse can be used to alter materials by ‘cold’ ablation (when a material is changed to gas directly from a solid) or to generate other colours/wavelengths through nonlinear frequency conversion. Diode-pumped solid-state lasers with high average power have produced femtosecond pulses with a pulse energy larger than 1  $\mu$ J with a 30 MHz pulse repetition rate. This is an unprecedented combination of short pulse, high pulse energy and high average power.

Such high peak intensity sources make ‘non-thermal’ ablation (without an increase in temperature) possible without any further amplification. The ability of intense ultrashort-pulse lasers to fabricate microstructures in solid targets is very promising, and the quality of ablated holes and patterns is much better using femtosecond or picosecond pulses instead of nanosecond pulses<sup>35–37</sup>. Ultrafast ‘non-thermal’ melting in semiconductors has been observed, where a solid-to-liquid phase transition occurs faster than carrier–lattice equilibration times<sup>38,39</sup>. This fast mode of material modification is important because it reduces undesirable effects caused by heat conduction and interaction of the pulse with ablated material. In medical applications, such short laser pulses have been used to obtain a higher level of surgical cutting precision, particularly in corneal surgery<sup>40</sup> and brain tumour removal<sup>41</sup>. These lasers reduce secondary damage effects, such as shock waves and cavitation bubbles, in tissues<sup>42</sup> because the fluence threshold for optical breakdown decreases with pulse duration<sup>43</sup>.

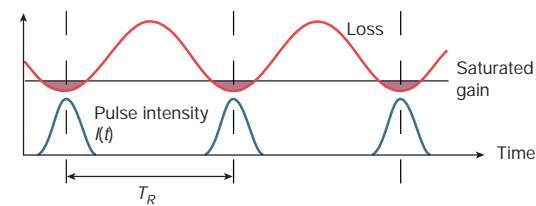
Simple external pulse compression combined with novel high average power solid-state lasers, at the full pulse repetition rate, results in peak powers as high as 12 MW with 33 fs pulses of the laser oscillator<sup>44</sup>. This pulse can be focused to a peak intensity of  $10^{14}$  W/cm<sup>2</sup>, a level at which high-field laser physics, such as high harmonic generation<sup>45,46</sup>

Box 1  
Modelocking

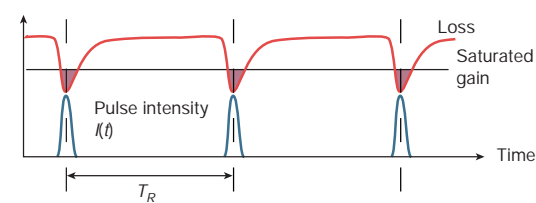
Modelocking is used to generate ultrashort pulses from lasers. A schematic set-up with a gain and a loss element inside a laser resonator is shown below. An output coupler partially transmits a small fraction of the laser pulse out of the laser resonator equally spaced by the resonator round-trip time. Typically an intracavity loss modulator is used to collect the laser light in short pulses around the minimum of the loss modulation with a period given by the cavity round-trip time  $T_R = 2L/v_g$ , where  $L$  is the laser cavity length and  $v_g$  the group velocity (that is, the propagation velocity of the peak of the pulse intensity). There are two type of modelocking: passive and active.



Active modelocking

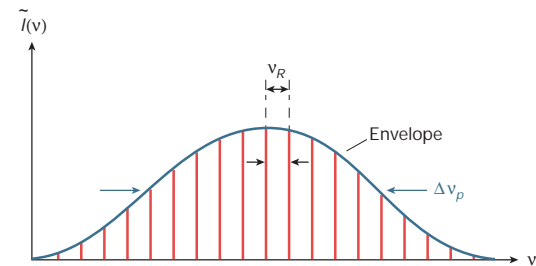
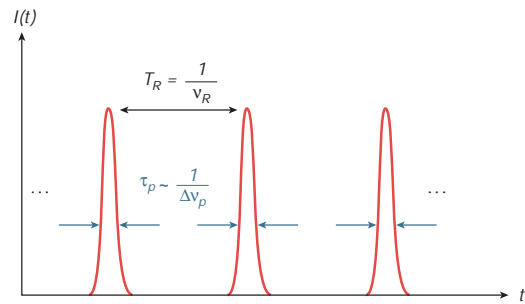


Passive modelocking



For active modelocking, an external signal is applied to an optical loss modulator typically using the acousto-optic or electro-optic effect. Such an electronically driven loss modulation produces a sinusoidal loss modulation with a period given by the cavity round-trip time  $T_R$ . The saturated gain at steady state then only supports net gain around the minimum of the loss modulation and therefore only supports pulses that are significantly shorter than the cavity round trip time.

For passive modelocking, a saturable absorber is used to obtain a self-amplitude modulation of the light inside the laser cavity. Such an absorber introduces some loss to the intracavity laser radiation, which is relatively large for low intensities but significantly smaller for a short pulse with high intensity. Thus, a short pulse then produces a loss modulation because the high intensity at the peak of the pulse saturates the absorber more strongly than its low intensity wings. This results in a loss modulation with a fast initial loss saturation (that is, reduction of the loss) determined by the pulse duration and typically a somewhat slower recovery that depends on the detailed mechanism of the absorption process in the saturable absorber. In effect, the circulating pulse saturates the laser gain to a level that is just sufficient to compensate for the losses from pulse itself, although any other circulating low-intensity light experiences more loss than gain and thus dies out during the following cavity round-trips. The obvious remaining question is how does passive modelocking start. Ideally, it starts from normal noise fluctuations in the laser. One noise spike is strong enough to significantly reduce its loss in the saturable absorber and thus will be more strongly amplified during the following cavity round trips, so that the stronger noise spike continues to further reduce its



loss and continues its growth until reaching steady state, where a stable pulse train has been formed.

Generally, we can obtain much shorter pulses with passive modelocking using a saturable absorber, because the recovery time of the saturable absorber can be very fast, resulting in a fast loss modulation. Modelocked pulses are much shorter than the cavity round-trip time and therefore can produce an ideal fast loss modulation that is inversely proportional to the pulse envelope. In comparison, any electronically driven loss modulation is significantly slower because of its sinusoidal loss modulation.

In the time domain, this means that a modelocked laser produces an equidistant pulse train, with a period defined by the round-trip time of a pulse inside the laser cavity  $T_R$  and a pulse duration  $\tau_p$ . In the frequency domain, this results in a phase-locked frequency comb with a constant mode spacing that is equal to the pulse repetition rate  $\nu_R = 1/T_R$ . The spectral width of the envelope of this frequency comb is inversely proportional to the pulse duration.

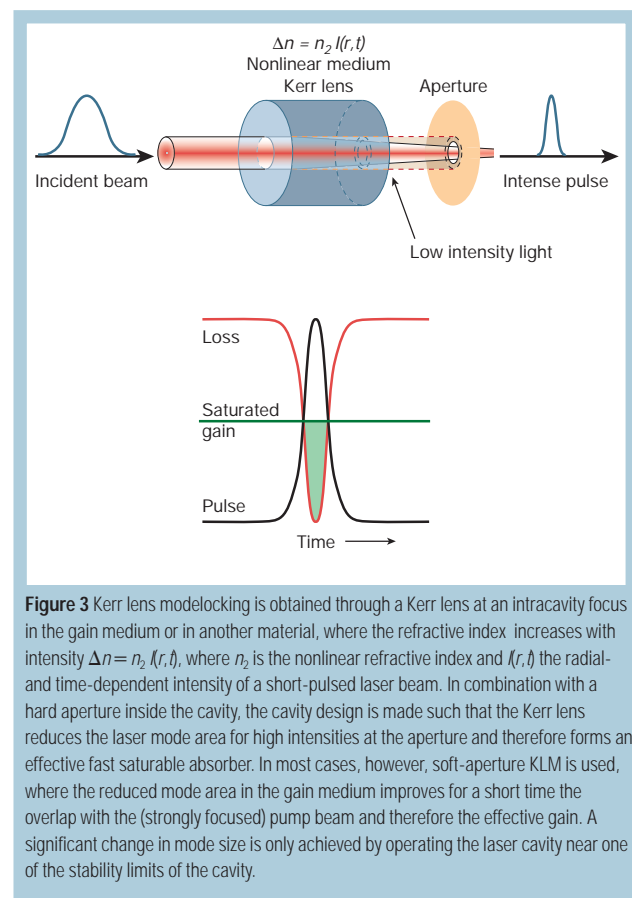


**Figure 3** Kerr lens modelocking is obtained through a Kerr lens in an intracavity focus in the gain medium or in another material, where the refractive index increases with intensity  $\Delta n = n_2 I(r, t)$ , where  $n_2$  is the nonlinear refractive index and  $I(r, t)$  the radial- and time-dependent intensity of a short-pulsed laser beam. In combination with a hard aperture inside the cavity, the cavity design is made such that the Kerr lens reduces the laser mode area for high intensities at the aperture and therefore forms an effective fast saturable absorber. In most cases, however, soft-aperture KLM is used, where the reduced mode area in the gain medium improves for a short time the overlap with the (strongly focused) pump beam and therefore the effective gain. A significant change in mode size is only achieved by operating the laser cavity near one of the stability limits of the cavity.

and laser plasma generated X-rays<sup>47</sup>, are possible. This increased pulse repetition rate would improve signal-to-noise ratios by four orders of magnitude compared with standard sources at kilohertz repetition rates. This is important for low-power applications such as X-ray imaging and microscopy<sup>48</sup>, femtosecond extreme UV and soft X-ray photoelectron spectroscopy<sup>49</sup> and ultrafast X-ray diffraction<sup>38,39</sup>.

I have outlined a few examples of ultrafast lasers, but many other applications already exist and many more will be developed in the future. Many of these applications are only possible because of the development of solid-state lasers and new modelocking techniques, particularly Kerr lens and semiconductor saturable absorber modelocking, which will be discussed next.

### Ti:sapphire laser and Kerr lens modelocking (KLM)

The success of passively modelocked dye lasers in the 70s and 80s<sup>50,51</sup> (Fig. 2) was partially due to the absence of the Q-switching problem present in solid-state lasers. These dye lasers were the first to generate sub-picosecond pulses<sup>52</sup> and were the workhorses of research laboratories for time-resolved spectroscopy. External pulse compression resulted in 6 fs pulses<sup>5</sup>—a record that lasted for 10 years.

In the late 80s, Ti:sapphire was a newly discovered solid-state laser material that had the necessary broad gain bandwidth to support femtosecond pulses<sup>54</sup>. By the end of the 80s, it was generally assumed that everything about modelocked Ti:sapphire lasers was understood, but there was a surprise to come. In 1990, two important papers were presented at consecutive conferences. First, Ishida *et al.*<sup>55</sup> presented a passively modelocked Ti:sapphire laser with an intracavity saturable absorber dye that produced stable 190 fs pulses. Second, Sibbett's group presented 60 fs pulses from a Ti:sapphire laser that appeared not to have a saturable absorber<sup>56</sup>. This second result—in the absence of a visible saturable absorber—had an instant impact on the research community, but the ultrafast laser experts realized that

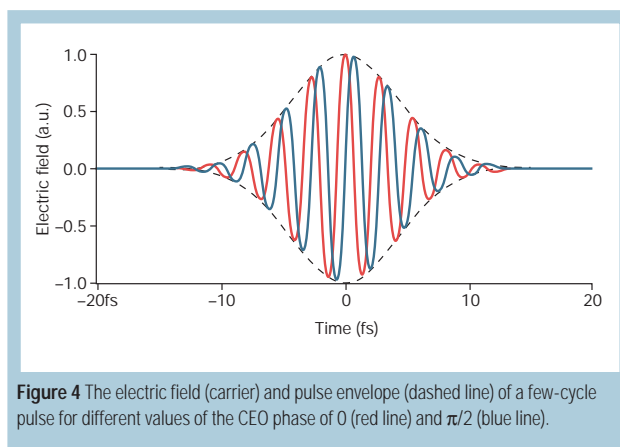


**Figure 4** The electric field (carrier) and pulse envelope (dashed line) of a few-cycle pulse for different values of the CEO phase of 0 (red line) and  $\pi/2$  (blue line).

the first result was also very surprising, even though a saturable absorber was present. It was clear that the dye saturable absorber, with a recovery time in the nanosecond range, could not support ultrashort pulses with a Ti:sapphire laser as it could with dye lasers. Sibbett's modelocking approach<sup>55,56</sup> was initially termed 'magic modelocking', and it triggered a major research effort into understanding passive modelocking of solid-state lasers. This form of modelocking was soon explained<sup>57–59</sup> and is now referred to as Kerr lens modelocking (KLM) (Fig. 3). Ishida's result was also explained by KLM: the slow dye saturable absorber only provided a reliable starting mechanism for KLM<sup>60</sup>.

KLM allowed the community to shorten pulses to the few femtosecond regime. Because the Kerr lens produces a 'non-resonant' saturable absorber, it is inherently broadband, broader than any other saturable absorber available today. With ultrafast dye lasers, pulses as short as 27 fs with around 10 mW average power were generated<sup>61</sup>, but pulses around 5–6 fs with around 100 mW average power can be produced with Ti:sapphire lasers<sup>62,63</sup>. In addition, very broad tunability with shorter than 100 fs pulses became possible for the first time. For time-resolved spectroscopy, these features had a major impact, because, for the first time, such lasers could be used on a wide range of materials.

KLM has some significant drawbacks. Generally, KLM lasers are not self-starting, that is, pulse formation does not start on its own, and additional perturbation to briefly increase laser noise is required. This is typically achieved by mechanically 'shaking' one of the laser cavity mirrors. Restrictive cavity designs<sup>64,65</sup> allow partial self-starting, but this generally requires submillimetre precision for cavity mirror alignments, a very clean environment to minimize intracavity losses and a laser cavity operated close to the stability limit. In addition, optimization of self-starting conflicts with achieving the shortest possible pulses, because, when the cavity is optimized, the Kerr effect is too strong for very short pulses to react sensitively to long pulses during the start-up phase. In the picosecond regime, KLM lasers tend to be less stable because the Kerr lens becomes too weak. Therefore, the search for alternative solutions for compact ultrafast lasers continued.

### Semiconductor saturable absorbers (SESAMs)

The breakthrough in the development of ultrafast lasers came with the semiconductor saturable absorber<sup>2</sup> (Box 2). In contrast to KLM lasers, the saturable absorber can be optimized independently of cavity design, allowing successful modelocking to be achieved with a broad range of solid-state lasers and cavity designs.

As early as 1974, a CO<sub>2</sub> laser<sup>66</sup>, and in 1980 and 1984, a semiconductor diode laser<sup>67</sup> and a colour center laser<sup>68</sup>, respectively, were passively modelocked with a semiconductor saturable absorber. In all these cases, the underlying physics of the modelocking process was significantly different from modelocking ion-doped solid-state

## Box 2

## Saturable absorbers and SESAMs

A saturable absorber is a material that has decreasing light absorption with increasing light intensity. We need saturable absorbers that show this effect at the intensities typically found in solid-state laser cavities, and semiconductor saturable absorbers are ideally suited for this. The key parameters for a saturable absorber are its wavelength range (where it absorbs), its dynamic response (how fast it recovers), and its saturation intensity and fluence (at what intensity or pulse energy density it saturates).

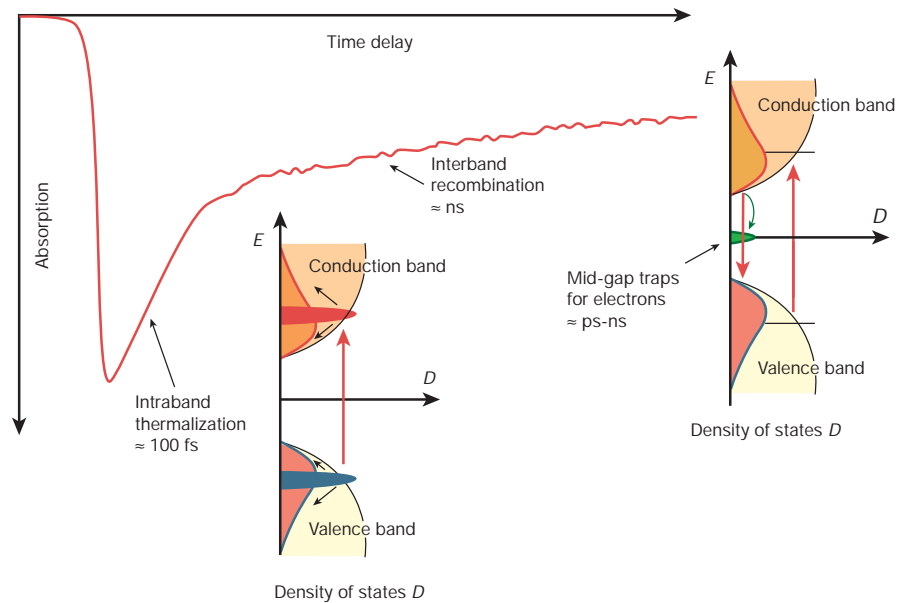
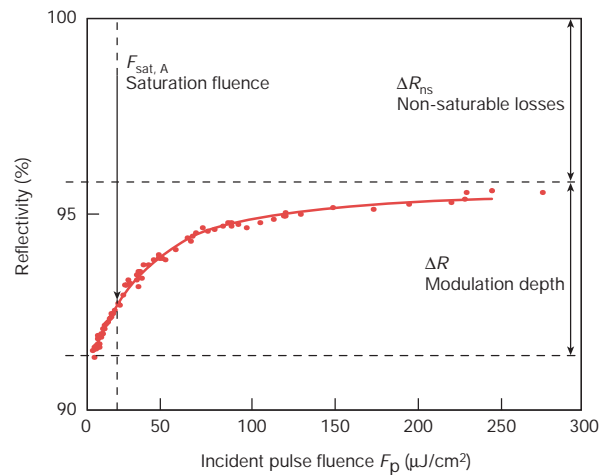
Saturable absorbers used in the past were typically dyes, which have short lifetimes, high toxicity and complicated handling procedures.

Alternative solid-state saturable absorbers include crystals such as Cr:YAG, which typically operate for only a limited range of wavelengths, recovery times and saturation levels.

Semiconductor materials, however, can absorb over a broad range of wavelengths (from the visible to the mid-infrared). We can also control their absorption recovery time and saturation fluence (typically 1 to 100  $\mu\text{J}/\text{cm}^2$ ) by altering the growth parameters and device design.

Semiconductor saturable absorbers are integrated into a mirror structure, resulting in a device that reflects more light the more intense the light is. We call this general class of device semiconductor saturable absorber mirrors—SESAMs. The SESAM is a saturable absorber that operates in reflection, thus the reflectivity increases with higher incoming pulses (see the figure on the right). During the past decade we have significantly improved the device design, fabrication process and long-term device reliability. We have SESAM designs that can cover wavelengths from <800 nm to >1600 nm, pulsewidths from femtoseconds to nanoseconds, and power levels from milliwatts to >100 watts.

A semiconductor absorbs light when the photon energy is sufficient to excite carriers from the valence band to the conduction band. Under conditions of strong excitation, the absorption is saturated because possible initial states of the pump transition are depleted while the final states are partially occupied. Within 60–300 fs of excitation, the carriers in each band thermalize, and this leads to a partial recovery of the absorption. On a longer time scale—typically between a few picoseconds and a few nanoseconds—the carrier will be removed by recombination and trapping. The presence of two different time scales can be rather useful for modelocking. The longer time constant results in a reduced saturation intensity for a part of the absorption, which facilitates self-starting modelocking, whereas the faster time constant is more effective in shaping subpicosecond pulses. Therefore, SESAMs allow us to easily obtain self-starting modelocking.



lasers such as Ti:sapphire, Nd:YAG, Yb:YAG, Cr:LiSAF and so on. The main difference is that these lasers have an emission cross-section that is typically more than 1,000 times smaller, and an upper state lifetime of the laser transition more than 1,000 times longer, than dye, diode and colour center lasers. The smaller the emission cross-section, the stronger the tendency for self-Q-switching (Box 3). This meant that the parameters of the saturable absorber had to be carefully adapted to prevent Q-switching instabilities, which partially explains why it took so long for the first successful demonstration. In addition, the theoretical background of Q-switched modelocking instabilities had not been fully worked out. Once this was under-

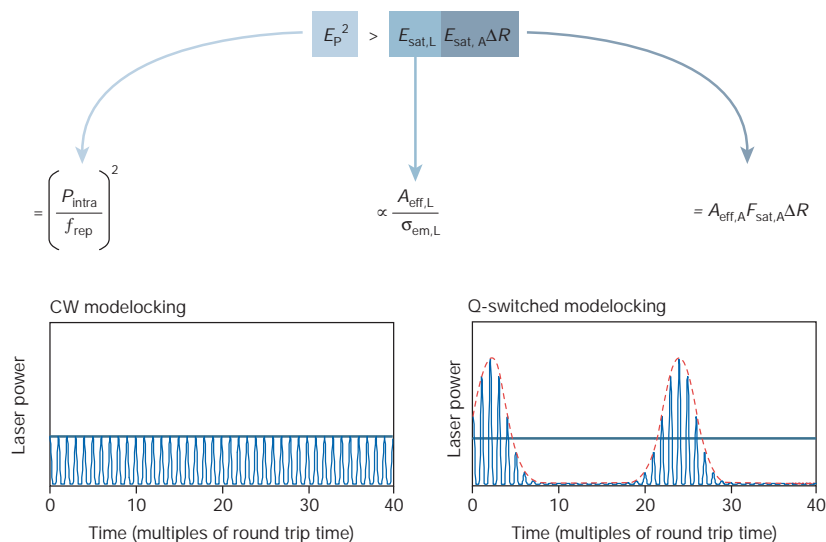
stood<sup>69</sup>, much better performance in terms of average output power and high pulse repetition rates was ultimately achieved.

Saturable absorbers with the parameters, such as modulation depth, saturation fluence and nonsaturable losses (Box 2), required for a given laser cavity and pump power were obtained using semiconductor mirror devices, where one or more semiconductor saturable absorber layers are embedded inside a mirror structure. Different semiconductor materials provide a wide range of bandgaps for operation from the visible to the far-infrared spectral range, therefore, bandgap engineering can provide broad tunability. In addition, defect engineering for recovery times ranging from the nanosecond to the

## Box 3

## Q-switched modelocking

A saturable absorber may also produce Q-switched modelocking, where the laser emits bunches of modelocked pulses, which may or may not have a stable Q-switching envelope. Q-switching instabilities occur when the pulse energy is temporarily increased because of noise fluctuations in the laser, which then gets even further increased because of the stronger saturation of the saturable absorber. This has to be balanced by a stronger saturation of the gain. If the gain is not sufficiently saturated then the pulse energy will increase further and self-Q-switching occurs. The physical background of Q-switching instabilities in ion-doped solid-state lasers can be prevented if  $E_p^2 > E_{\text{sat,L}} E_{\text{sat,A}} \Delta R$ , assuming that the saturable absorber is fully saturated.



The important parameters are  $E_p$  intracavity energy,  $P_{\text{intra}}$  intracavity average power,  $f_{\text{rep}}$  pulse repetition rate,  $E_{\text{sat,L}}$  saturation energy of the laser medium,  $A_{\text{eff,L}}$  average mode area inside the laser medium,  $\sigma_{\text{em,L}}$  emission cross-section of gain material,  $E_{\text{sat,A}}$  saturation energy of the absorber,  $A_{\text{eff,A}}$  average mode area inside the saturable absorber,  $F_{\text{sat,A}}$  saturation fluence of absorber,  $\Delta R$  modulation depth of the saturable absorber.

For femtosecond pulses, modelocking can be further supported by soliton formation, which relaxes the critical intracavity pulse energy by a factor of three to 10, depending on the specific parameters.

femtosecond regime is possible. Saturable absorbers can be adjusted to the required absorber parameter even when the mode size is fixed.

Typically the SESAM is operated with an incident pulse fluence of about three to five times that of the saturation fluence. This saturation level of the absorber provides nearly the maximum modulation depth without damaging the device<sup>70</sup>. Higher saturation also reduces the tendency for Q-switching instabilities because of thermal effects and two-photon absorption, which becomes more significant for femtosecond pulses. The recovery time of the SESAM can be as long as 10 to 30 times relative to the final pulse duration<sup>70</sup>, and with this form of modelocking, pulses as short as 13 fs have been generated<sup>71</sup>.

The success of semiconductor saturable absorbers for passively modelocked solid-state lasers results from their small saturation fluence and the additional benefits of cavity mirror device integration, sophisticated bandgap and defect engineering and epitaxial wafer-scale fabrication, which reduces its production cost substantially. SESAM design depends strongly on the laser parameters and can be optimized for different operational regimes. On the basis of KLM and SESAMs, the performance frontiers of pulsed solid-state lasers have been pushed forward by orders of magnitude during the past decade. These fast moving frontiers in pulse duration, average power and pulse repetition rate will be discussed next.

### Frontiers: ultrashort pulses

At present, nothing is better than the Ti:sapphire laser as an ultrafast laser. Only KLM Ti:sapphire lasers have generated less than 6 fs pulse durations<sup>62,72</sup>. At a centre wavelength of 800 nm, an optical cycle lasts only 2.7 fs; therefore, a pulse duration of 5.4 fs has only two optical cycles at full-width half-maximum of the pulse intensity. Significantly shorter pulses have only been generated using pulse compression in noble-gas-filled hollow fibres<sup>73</sup> or with synchronously pumped optical parametric oscillators<sup>74</sup>. At the moment, the shortest pulses that are properly and fully characterized by an indepen-

dent phase measurement<sup>75</sup> in the visible and near-infrared spectral regime are 3.8 fs long<sup>76</sup>. In this regime, the measurement of pulse duration is nearly as difficult as generating them. Unfortunately, new record pulses have been claimed without them being properly measured, because, generally, less careful measurement results in a 'shorter pulse'.

Dispersion management is an increasingly hard task in the few-cycle regime. Generally, when a pulse propagates through a medium it acquires a frequency-dependent phase shift and broadens. Dispersive pulse broadening is a linear effect and therefore can be compensated for by rearranging the different spectral components in time at a different place inside the laser cavity. Non-absorbing materials generally exhibit positive dispersion, and regrouping the different spectral components requires the opposite frequency-dependent phase shift (that is, negative dispersion).

Negative dispersion with low losses is typically obtained using geometrical effects, such as inserting a pair of prisms into the cavity<sup>78</sup>, where different wavelength components will travel on slightly different optical paths. The negative dispersion obtained from this effect is proportional to the prism separation, and a positive dispersion results from propagation in the prism, but this is easily adjusted by altering how much of the prism is inserted into the optical path. However, residual higher-order dispersion normally limits the pulse duration in Ti:sapphire lasers to about 10 fs using fused quartz prism pairs<sup>79–81</sup>.

Dielectric Bragg mirrors with regular quarter-wave stacks of alternating materials with high and low refractive indices have a negligibly small dispersion when operated within their reflection bandwidth but an increasing dispersion at the edges of this range. Modified designs can be used to obtain well controlled dispersion over a large wavelength range with chirped mirrors<sup>82</sup>, which give a much broader reflection bandwidth than any other mirror. With chirped mirrors, less than 10 fs pulses have been generated with good quality for the first time<sup>83</sup>, and further improvements in chirped mirror designs, such as double

chirped mirrors<sup>84,85</sup> and back-side coated chirped mirrors<sup>86</sup>, have resulted in record pulsewidth results<sup>87</sup>.

Ultrashort pulses in the one-to-two optical cycle regime also open up new possibilities in nonlinear optics, where the variation in electric field strength becomes significant for different carrier envelope offset (CEO) phases (Fig. 4). Inside a femtosecond laser oscillator, no coupling mechanism exists between the propagation speeds of the carrier and the pulse envelope. Therefore, the relative delay between the carrier and the envelope of a femtosecond oscillator will exhibit irregular fluctuations unless this jitter is actively suppressed. Different techniques have been proposed to stabilize the CEO frequency in the time domain<sup>88</sup> and in the frequency domain<sup>30</sup>. The frequency domain technique is much more sensitive and is generally the technique that is used<sup>89,90</sup>. We have achieved a long-term CEO stabilization with a residual 10 as timing jitter, which corresponds to 0.025 rad rms CEO phase noise<sup>31</sup>. Applications of CEO nonlinear optics in photoelectron emission<sup>32</sup>, high harmonic generation<sup>33</sup> and attosecond pulse generation have shown very interesting results<sup>34</sup>.

### Frontier: high average power

Diode-pumped CW lasers could generate hundreds of watts or even kilowatts by the early 1990s; however, the output power of mode-locked diode-pumped lasers was still limited to ~100 mW. Only in recent years has this limit increased to 60 W in femtosecond pulses<sup>9</sup>. In terms of pulse energies, 100 mW average output power at a pulse repetition rate of 100 MHz corresponds to 1 nJ of pulse energy. This has been surpassed by three orders of magnitude: the 60 W laser produced nearly 2  $\mu$ J pulse energy directly from a SESAM modelocked diode-pumped solid-state laser both in the pico- and femtosecond pulse regime. With external pulse compression, peak powers as high as 12 MW have been generated, as described earlier. In addition, a synchronously pumped fibre-feedback optical parametric oscillator (OPO)<sup>91</sup>, a novel type of high-gain synchronously pumped OPO that is particularly insensitive to cavity losses and drifts of the cavity length, produced up to 15 W in 700 fs pulses. OPOs are attractive sources of broadly wavelength-tunable ultrashort pulses, which are required for many applications, for example, RGB display systems.

Initial attempts to obtain higher powers from modelocked lasers had problems, for example, high power scaling was restricted by the requirement to maintain fundamental Gaussian beam quality and to suppress Q-switching instabilities<sup>92</sup>. Many high-power laser heads have large mode areas in the laser gain medium. This often results from the poor beam quality of high-power diode bars. Although for CW lasers this is no problem, it leads to excessive Q-switching instabilities in a passively modelocked laser (Box 3). Thus, more stringent requirements are set for the SESAM design. This is one reason why power scaling typically comes at the expense of longer pulses, because the modulation depth of the SESAM has to be reduced. So far, the best laser head for power scaling of passively modelocked diode-pumped solid-state lasers is based on a thin-disk laser<sup>93</sup> and utilizes a disk of, for example, Yb:YAG directly attached to a water-cooled mount. Thermal limitations are minimized by using a disk thickness of 100–250  $\mu$ m. Efficient pump absorption in a thin disk is achieved by using multiple (for example, up to 32) passes of the pump radiation. Today, such thin disk lasers are commercially available with more than 1 kW average power. So far Gaussian beam quality has only been demonstrated with up to 100 W of average power, but hundreds of watts should be possible. This combination of SESAM-modelocked thin-disk laser is scalable: the main challenges (beam quality, Q-switching instabilities and SESAM damage) do not become more severe if the power is scaled up. Therefore, the 60 W average power will not remain an upper limit.

### Frontier: high pulse repetition rate

Q-switching instabilities limited the highest pulse repetition rates in passively modelocked diode-pumped solid-state lasers to 1 GHz for a long time. For the first time, pulse repetition rates above 10 GHz from

passively modelocked ion-doped solid-state lasers have been generated with Nd:YVO<sub>4</sub> lasers at a centre wavelength around 1  $\mu$ m<sup>94</sup>. Shortly afterwards this was increased to 77 GHz<sup>95</sup> and 160 GHz<sup>7</sup>. Average power has been optimized at a 10 GHz pulse repetition rate to 2.1 W<sup>7</sup>. The peak power was sufficient for efficient nonlinear frequency conversion. For example, a synchronously pumped OPO was demonstrated that produced picosecond pulses that were broadly tunable around 1.55  $\mu$ m with up to 100 mW average output power<sup>96</sup>.

Diode-pumped Er:Yb:glass is well suited for telecom applications. Its gain bandwidth covers the entire C-band, it can be pumped with standard 980 nm laser diodes used in erbium-doped fibre amplifiers, and it is robust and inexpensive. However, its small emission cross-section typically prevents high repetition rates without Q-switched modelocking. Using SESAM design optimization this limitation was overcome, and tunable picosecond pulses at 10 GHz<sup>19</sup>, 25 GHz<sup>25</sup> and 40 GHz<sup>20</sup> have been generated.

Actively modelocked fibre lasers can generate pulse repetition rates up to 200 GHz<sup>97</sup> but only with harmonic modelocking, where multiple pulses circulate in the laser cavity instead of one (Box 1). Good pulse stability is then only achieved by using quite complex means for stabilization. We prefer the simpler approach of fundamental modelocking, that is, with only a single pulse circulating in the laser cavity.

Edge-emitting semiconductor lasers, passively or actively mode-locked, can generate repetition rates of more than 1 THz<sup>98</sup>, but have a fairly limited average output power because of the limited mode area. Optically pumped vertical-external cavity surface-emitting lasers (VECSELs) have been passively modelocked with an intracavity saturable absorber<sup>99</sup>. Average power scaling is not limited, and 950 mW of average power in 15 ps pulses with a 6 GHz repetition rate<sup>100</sup> has been generated, with the promise of even higher powers in the multi-gigahertz regime.

The progress in ultrafast compact lasers during the past decade has been simply amazing. The good news is that I strongly believe that this will not be the end of the story. I expect further power scaling to more than 100 W of average power and more compact and cheaper lasers that will support more widespread use for many different applications. □

doi:10.1038/nature01938

1. Maria, A. J. D., Stetser, D. A. & Heynau, H. Self mode-locking of lasers with saturable absorbers. *Appl. Phys. Lett.* **8**, 174–176 (1966).
2. Keller, U. *et al.* Solid-state low-loss intracavity saturable absorber for Nd:YLF lasers: an antiresonant semiconductor Fabry-Perot saturable absorber. *Opt. Lett.* **17**, 505–507 (1992).
3. Keller, U. *et al.* Semiconductor saturable absorber mirrors (SESAMs) for femtosecond to nanosecond pulse generation in solid-state lasers. *IEEE J. Sel. Top. Quantum Electron.* **2**, 435–453 (1996).
4. Keller, U. in *Nonlinear Optics in Semiconductors* (eds Garmire, E. & Kost, A.) 211–286 (Academic Press, Boston, 1999).
5. Spence, D. E., Kean, P. N. & Sibbett, W. 60-fsec pulse generation from a self-mode-locked Ti:sapphire laser. *Opt. Lett.* **16**, 42–44 (1991).
6. Innerhofer, E. *et al.* 60 W average power in 810-fs pulses from a thin-disk Yb:YAG laser. *Opt. Lett.* **28**, 367–369 (2003).
7. Kraimer, L. *et al.* Compact Nd:YVO<sub>4</sub> lasers with pulse repetition rates up to 160 GHz. *IEEE J. Quantum Electron.* **38**, 1331–1338 (2002).
8. Shah, J. *Ultrafast spectroscopy of semiconductors and semiconductor nanostructures* (Springer-Verlag, Berlin, 1996).
9. Zewail, A. H. Femtochemistry: Recent progress in studies of dynamics and control of reactions and their transition states. *J. Phys. Chem.* **100**, 12701 (1996).
10. Zewail, A. H. Femtochemistry: atomic-scale dynamics of chemical bond. *J. Phys. Chem. A* **104**, 5660–5694 (2000).
11. Valdmantis, J. A. & Mourou, G. A. Subpicosecond electrooptic sampling: principles and applications. *IEEE J. Quantum Electron.* **22**, 69–78 (1986).
12. Weingarten, K. J., Rodwell, M. J. W. & Bloom, D. M. Picosecond optical sampling of GaAs integrated circuits. *IEEE J. Quantum Electron.* **24**, 198–220 (1988).
13. Ramaswami, R. & Sivarajan, K. *Optical Networks: A Practical Perspective* (Morgan Kaufmann, 1998).
14. Mollenauer, L. F. *et al.* Demonstration of massive wavelength-division multiplexing over transoceanic distances by use of dispersion-managed solitons. *Opt. Lett.* **25**, 704–706 (2000).
15. Miller, D. A. B. Optical interconnects to silicon. *IEEE J. Sel. Top. Quantum Electron.* **6**, 1312–1317 (2000).
16. Krishnamoorthy, A. V. & Miller, D. A. B. Scaling optoelectronic-VLSI circuits into the 21st century: a technology roadmap. *IEEE J. Sel. Top. Quantum Electron.* **2**, 55–76 (1996).
17. Hatziefremidis, A., Papadopoulos, D. N., Fraser, D. & Avramopoulos, H. Laser sources for polarized electron beams in cw and pulsed accelerators. *Nucl. Instrum. Meth. A* **431**, 46–52 (1999).
18. Mollenauer, L. F. & Mamyshv, P. V. Massive wavelength-division multiplexing with solitons. *IEEE J. Quantum Electron.* **34**, 2089–2102 (1998).
19. Kraimer, L. *et al.* Tunable picosecond pulse-generating laser with a repetition rate exceeding 10 GHz.

- Electron. Lett.* **38**, 225–227 (2002).
20. Zeller, S. C. *et al.* Passively mode-locked 40-GHz Er:Yb-glass laser. *Appl. Phys. B* **76**, 787–788 (2003).
  21. Huang, D. *et al.* Optical coherence tomography. *Science* **254**, 1178–1181 (1991).
  22. Fujimoto, J. G. Optical coherence tomography. *C. R. Acad. Sci. Paris Serie IV* **2**, 1099–1111 (2001).
  23. Boivin, L., Wegmueller, M., Nuss, M. C. & Knox, W. H. 110 Channels x 2.35 Gb/s from a single femtosecond laser. *IEEE Photonics Technology Lett.* **11**, 466–468 (1999).
  24. Souza, E. A. D., Nuss, M. C., Knox, W. H. & Miller, D. A. B. Wavelength-division multiplexing with femtosecond pulses. *Opt. Lett.* **20**, 1166–1168 (1995).
  25. Spühler, G. J. *et al.* Novel multi-wavelength source with 25-GHz channel spacing tunable over the C-band. *Electron. Lett.* **39**, 778–780 (2003).
  26. Holzwarth, R. *et al.* Optical frequency synthesizer for precision spectroscopy. *Phys. Rev. Lett.* **85**, 2264–2267 (2000).
  27. Holzwarth, R., Zimmermann, M., Udem, T. & Hänsch, T. W. Optical clockworks and the measurement of laser frequencies with a mode-locked frequency comb. *IEEE J. Quantum Electron.* **37**, 1493–1501 (2001).
  28. Stenger, J. *et al.* Phase-coherent frequency measurement of the Ca intercombination line at 657 nm with a Kerr-lens mode-locked femtosecond laser. *Phys. Rev. A* **63**, 021802 (2001).
  29. Udem, T., Holzwarth, R. & Hänsch, T. W. Optical frequency metrology. *Nature* **416**, 233–237 (2002).
  30. Telle, H. R. *et al.* Carrier-envelope offset phase control: A novel concept for absolute optical frequency measurement and ultrashort pulse generation. *Appl. Phys. B* **69**, 327–332 (1999).
  31. Helbing, F. W., Steinmeyer, G., Stenger, J., Telle, H. R. & Keller, U. Carrier-envelope-offset dynamics and stabilization of femtosecond pulses. *Appl. Phys. B* **74**, S35–S42 (2002).
  32. Paulus, G. G. *et al.* Absolute-phase phenomena in photoionization with few-cycle laser pulses. *Nature* **414**, 182–184 (2001).
  33. Baltuska, A. *et al.* Attosecond control of electronic processes by intense light fields. *Nature* **421**, 611–615 (2003).
  34. Drescher, M. *et al.* X-ray pulses approaching the attosecond frontier. *Science* **291**, 1923–1927 (2001).
  35. Liu, X., Du, D. & Mourou, G. Laser ablation and micromachining with ultrashort laser pulses. *IEEE J. Quantum Electron.* **33**, 1706–1716 (1997).
  36. Nolte, S. *et al.* Ablation of metals by ultrashort laser pulses. *J. Opt. Soc. Am. B* **14**, 2716–2722 (1997).
  37. von der Linde, D., Sokolowski-Tinten, K. & Bialkowski, J. Laser-solid interaction in the femtosecond time regime. *Appl. Surf. Sci.* **109/110**, 1–10 (1997).
  38. Siders, C. W. *et al.* Detection of nonthermal melting by ultrafast X-ray diffraction. *Science* **286**, 1340–1342 (1999).
  39. Rousse, A. *et al.* Non-thermal melting in semiconductors measured at femtosecond resolution. *Nature* **410**, 65–68 (2001).
  40. Loesel, F. H., Niemz, M. H., Bille, J. F. & Juhasz, T. Laser-induced optical breakdown on hard and soft tissues and its dependence on the pulse duration: experiment and model. *IEEE J. Quantum Electron.* **32**, 1717–1722 (1996).
  41. Hammer, D. X. *et al.* Experimental investigation of ultrashort pulse laser induced breakdown thresholds in aqueous media. *IEEE J. Quantum Electron.* **32**, 670–678 (1996).
  42. Juhasz, T. *et al.* Corneal refractive surgery with femtosecond lasers. *IEEE J. Sel. Top. Quantum Electron.* **5**, 902–910 (1999).
  43. Loesel, F. H. *et al.* Non-thermal ablation of neural tissue with femtosecond laser pulses. *Appl. Phys. B* **66**, 121–128 (1998).
  44. Südmeyer, T. *et al.* Nonlinear femtosecond pulse compression at high average power levels using a large area holey fiber. *Opt. Lett.* (in the press).
  45. Ferray, M. *et al.* Multiple-harmonic conversion of 1064 nm radiation in rare gases. *J. Phys. B: At. Mol. Opt. Phys.* **21**, L31–L35 (1988).
  46. Levenstein, M., Balcou, P., Ivanov, M. Y., L'Huillier, A. & Corkum, P. B. Theory of high-harmonic generation by low-frequency laser fields. *Phys. Rev. A* **49**, 2117–2132 (1994).
  47. Murnane, M. M., Kapteyn, H. C., Rosen, M. D. & Falcone, R. W. Ultrafast X-Ray pulses from laser-produced plasmas. *Science* **251**, 531–536 (1991).
  48. Schmidt, O. *et al.* Time-resolved two-photon photoemission electron microscopy. *Appl. Phys. B* **74**, 223–227 (2002).
  49. Bauer, M. *et al.* Direct observation of surface chemistry using ultrafast soft-X-ray pulses. *Phys. Rev. Lett.* **87**, 025501 (2001).
  50. Shank, C. V. in *Ultrashort Laser Pulses and Applications* (ed. Kaiser, W.) Chapter 2 (Springer, Heidelberg, 1988).
  51. Diels, J.-C. in *Dye lasers principles: with applications* (eds Duarte, F. J. and Hillman, L. W.) 41–132 (Academic Press, Boston, 1990).
  52. Shank, C. V. & Ippen, E. P. Subpicosecond kilowatt pulses from a modelocked cw dye laser. *Appl. Phys. Lett.* **24**, 373–375 (1974).
  53. Fork, R. L., Cruz, C. H. B., Becker, P. C. & Shank, C. V. Compression of optical pulses to six femtoseconds by using cubic phase compensation. *Opt. Lett.* **12**, 483–485 (1987).
  54. Moulton, P. F. Spectroscopic and laser characteristics of Ti:Al<sub>2</sub>O<sub>3</sub>. *J. Opt. Soc. Am. B* **3**, 125–132 (1986).
  55. Ishida, Y., Sarukura, N. & Nakano, H. in *Ultrafast Phenomena PD11-11* (OSA, California, 1990).
  56. Spence, D. E., Kean, P. N. & Sibbett, W. in *Conference on Lasers and Electro-optics (CLEO) CPDP10* (OSA/IEEE LEOS, Anaheim, California, 1990).
  57. Keller, U., 'tHooft, G. W., Knox, W. H. & Cunningham, J. E. Femtosecond pulses from a continuously self-starting passively mode-locked Ti:Sapphire laser. *Opt. Lett.* **16**, 1022–1024 (1991).
  58. Salin, F., Squier, J. & Piché, M. Modelocking of Ti:Sapphire lasers and self-focusing: a Gaussian approximation. *Opt. Lett.* **16**, 1674–1676 (1991).
  59. Negus, D. K., Spinelli, L., Goldblatt, N. & Feugnet, G. in *Advanced Solid-State Lasers* (eds Dubé, G. & Chase, L.) 120–124 (Optical Society of America, Washington D.C., 1991).
  60. Keller, U., Knox, W. H. & 'tHooft, G. W. Ultrafast solid-state mode-locked lasers using resonant nonlinearities. *IEEE J. Quantum Electron.* **28**, 2123–2133 (1992).
  61. Valdmanis, J. A. & Fork, R. L. Design considerations for a femtosecond pulse laser balancing self phase modulation, group velocity dispersion, saturable absorption, and saturable gain. *IEEE J. Quantum Electron.* **22**, 112–118 (1986).
  62. Sutter, D. H. *et al.* Semiconductor saturable-absorber mirror-assisted Kerr-lens mode-locked Ti:Sapphire laser producing pulses in the two-cycle regime. *Opt. Lett.* **24**, 631–633 (1999).
  63. Ell, R. *et al.* Generation of 5-fs pulses and octave-spanning spectra directly from a Ti:Sapphire laser. *Opt. Lett.* **26**, 373–375 (2001).
  64. Cerullo, G., De Silvestri, S., Magni, V. & Pallaro, L. Resonators for Kerr-lens mode-locked femtosecond Ti:Sapphire lasers. *Opt. Lett.* **19**, 807–809 (1994).
  65. Cerullo, G., De Silvestri, S. & Magni, V. Self-starting Kerr lens mode-locking of a Ti:Sapphire laser. *Opt. Lett.* **19**, 1040–1042 (1994).
  66. Gibson, A. F., Kimmitt, M. F. & Norris, B. Generation of bandwidth-limited pulses from a TEA CO<sub>2</sub> laser using p-type germanium. *Appl. Phys. Lett.* **24**, 306–307 (1974).
  67. Ippen, E. P., Eichenberger, D. J. & Dixon, R. W. Picosecond pulse generation by passive modelocking of diode lasers. *Appl. Phys. Lett.* **37**, 267–269 (1980).
  68. Islam, M. N. *et al.* Color center lasers passively mode locked by quantum wells. *IEEE J. Quantum Electron.* **25**, 2454–2463 (1989).
  69. Hönninger, C., Paschotta, R., Morier-Genouf, F., Moser, M. & Keller, U. Q-switching stability limits of continuous-wave passive mode locking. *J. Opt. Soc. Am. B* **16**, 46–56 (1999).
  70. Paschotta, R. & Keller, U. Passive mode locking with slow saturable absorbers. *Appl. Phys. B* **73**, 653–662 (2001).
  71. Kärtner, F. X., Jung, I. D. & Keller, U. Soliton Modelocking with Saturable Absorbers. *IEEE J. Sel. Top. Quantum Electron.* **2**, 540–556 (1996).
  72. Ell, R. *et al.* Generation of 5-fs pulses and octave-spanning spectra directly from a Ti:Sapphire laser. *Opt. Lett.* **26**, 373–375 (2001).
  73. Nisoli, M. *et al.* Compression of high energy laser pulses below 5 fs. *Optics Lett.* **22**, 522–524 (1997).
  74. Shirakawa, A., Sakane, I., Takasaka, M. & Kobayashi, T. Sub-5-fs visible pulse generation by pulse-front-matched noncollinear optical parametric amplification. *Appl. Phys. Lett.* **74**, 2268–2270 (1999).
  75. Gallmann, L. *et al.* Characterization of sub-6-fs optical pulses with spectral phase interferometry for direct electric-field reconstruction. *Opt. Lett.* **24**, 1314–1316 (1999).
  76. Schenkel, M. *et al.* Generation of 3.8-fs pulses from adaptive compression of a cascaded hollow fiber supercontinuum. *Opt. Lett.* (in the press).
  77. Gallmann, L., Sutter, D. H., Matuschek, N., Steinmeyer, G. & Keller, U. Techniques for the characterization of sub-10-fs optical pulses: a comparison. *Appl. Phys. B* **70**, S67–S75 (2000).
  78. Fork, R. L., Martinez, O. E. & Gordon, J. P. Negative dispersion using pairs of prisms. *Opt. Lett.* **9**, 150–152 (1984).
  79. Asaki, M. T. *et al.* Generation of 11-fs pulses from a self-mode-locked Ti:Sapphire laser. *Opt. Lett.* **18**, 977–979 (1993).
  80. Curley, P. F. *et al.* Operation of a femtosecond Ti:Sapphire solitary laser in the vicinity of zero group-delay dispersion. *Opt. Lett.* **18**, 54–56 (1993).
  81. Zhou, J. *et al.* Pulse evolution in a broad-bandwidth Ti:Sapphire laser. *Opt. Lett.* **19**, 1149–1151 (1994).
  82. Szipöcs, R., Ferencz, K., Spielmann, C. & Krausz, F. Chirped multilayer coatings for broadband dispersion control in femtosecond lasers. *Opt. Lett.* **19**, 201–203 (1994).
  83. Stingl, A., Lenzner, M., Ch. Spielmann, Krausz, F. & Szipöcs, R. Sub-10-fs mirror-dispersion-controlled Ti:Sapphire laser. *Opt. Lett.* **20**, 602–604 (1995).
  84. Kärtner, F. X. *et al.* Design and fabrication of double-chirped mirrors. *Opt. Lett.* **22**, 831–833 (1997).
  85. Matuschek, N., Kärtner, F. X. & Keller, U. Analytical design of double-chirped mirrors with custom-tailored dispersion characteristics. *IEEE J. Quantum Electron.* **35**, 129–137 (1999).
  86. Matuschek, N., Gallmann, L., Sutter, D. H., Steinmeyer, G. & Keller, U. Back-side coated chirped mirror with ultra-smooth broadband dispersion characteristics. *Appl. Phys. B* **71**, 509–522 (2000).
  87. Steinmeyer, G., Sutter, D. H., Gallmann, L., Matuschek, N. & Keller, U. Frontiers in ultrashort pulse generation: pushing the limits in linear and nonlinear optics. *Science* **286**, 1507–1512 (1999).
  88. Xu, L. *et al.* Route to phase control of ultrashort light pulses. *Opt. Lett.* **21**, 2008–2010 (1996).
  89. Jones, D. J. *et al.* Carrier-envelope phase control of femtosecond mode-locked lasers and direct optical frequency synthesis. *Science* **288**, 635–639 (2000).
  90. Apolonski, A. *et al.* Controlling the phase evolution of few-cycle light pulses. *Phys. Rev. Lett.* **85**, 740 (2000).
  91. Südmeyer, T. *et al.* Femtosecond fiber-feedback OPO. *Opt. Lett.* **26**, 304–306 (2001).
  92. Paschotta, R. *et al.* Diode-pumped passively mode-locked lasers with high average power. *Appl. Phys. B* **70**, S25–S31 (2000).
  93. Giesen, A. *et al.* Scalable concept for diode-pumped high-power solid-state lasers. *Appl. Phys. B* **58**, 363–372 (1994).
  94. Krainer, L. *et al.* Passively mode-locked Nd:YVO<sub>4</sub> laser with up to 13 GHz repetition rate. *Appl. Phys. B* **69**, 245–247 (1999).
  95. Krainer, L., Paschotta, R., Moser, M. & Keller, U. 77 GHz soliton modelocked Nd:YVO<sub>4</sub> laser. *Electron. Lett.* **36**, 1846–1848 (2000).
  96. Lecomte, S. *et al.* Optical parametric oscillator with 10 GHz repetition rate and 100 mW average output power in the 1.5-mm spectral region. *Opt. Lett.* **27**, 1714–1717 (2002).
  97. Yoshida, E. & Nakazawa, M. 80–200GHz erbium doped fiber laser using a rational harmonic mode-locking technique. *Electron. Lett.* **32**, 1370–1372 (1996).
  98. Arahira, S., Matsui, Y. & Ogawa, Y. Mode-locking at very high repetition rates more than terahertz in passively mode-locked distributed-Bragg-reflector laser diodes. *IEEE J. Quantum Electron.* **32**, 1211–1224 (1996).
  99. Hoogland, S. *et al.* Passively mode-locked diode-pumped surface-emitting semiconductor laser. *IEEE Photon. Technol. Lett.* **12**, 1135–1138 (2000).
  100. Häring, R. *et al.* High-power passively mode-locked semiconductor lasers. *IEEE J. Quantum Electron.* **38**, 1268–1275 (2002).

**Acknowledgements** I would like to acknowledge many important contributions from my graduate students, post-docs and collaborators. I would like to mention Rüdiger Paschotta, Günter Steinmeyer, Franz Kärtner, Markus Haiml who have been senior researchers and project leaders in my group at different times during the last 10 years and Kurt Weingarten, Gabriel Spühler and Lukas Krainer from GigaTera Inc. on the most recent work on high pulse repetition rate lasers. This work has been supported by ETH, the Swiss National Science Foundation (SNF) and the Swiss Technology and Innovation Foundation (KTI).